Magnetic Vibration Analysis of a New DC-Excited Multitoothed Switched Reluctance Machine

Chunhua Liu[1], K. T. Chau[1], *Fellow, IEEE*, Christopher H. T. Lee[1], Fei Lin[1], Fuhua Li[1], and T. W. Ching[2]

[1]Department of Electrical and Electronic Engineering, University of Hong Kong, Hong Kong
[2]Faculty of Science and Technology, University of Macau, Macau, China

This paper proposes a combined numerical and analytical approach for magnetic vibration analysis of a new dc-excited multitoothed switched reluctance (MSR) machine. First, the machine design is artfully to incorporate the dc-excited winding into the MSR topology, hence breeding a new flux controllable, high-torque, low-torque ripple, and doubly salient magnetless machine. Then, the finite-element-method is used to calculate the machine force and torque. A series of analytical equations are formulated to calculate the magnetic vibration parameters of the proposed machine. The analysis process and the corresponding results are given to verify the validity of the proposed approach for magnetic vibration analysis of the new machine.

***Index Terms*—Doubly salient machine, flux control, magnetic vibration, magnetless, noise analysis, switched reluctance machine.**

I. Introduction

DOUBLY salient magnetless (DSM) machine are re-attractive in recent years, owing to their cost benefit and acceptable performances [1]–[3]. But this kind of DSM machines has two obvious disadvantages, namely the torque ripple and noise, which greatly limit their applications [4]–[6].

The acoustic noise in DSM machines can be divided into two types: magnetic and mechanical [7]. The corresponding mechanical noise greatly depends on the machine installation and other mechanical factors. The corresponding magnetic noise comes from the radial magnetic attraction between the stator and rotor poles, which is independent of the torque ripple and cogging torque [7], [8]. This attractive force dominates the vibration and hence the machine magnetic noise.

This paper investigates the magnetic vibration and noise of a new kind of DSM machines, namely the dc-excited multitoothed switched reluctance (dc-MSR) machine. First, the machine design is to incorporate the dc-exited winding into the MSR structure, hence breeding a new flux controllable, high-torque and low-torque ripple DSM machine. Then, the time-stepping finite-element method (TS-FEM) is adopted to calculate the machine force, torque, and other performances. Then, a series of analytical equations are formulated to calculate the magnetic vibration parameters of the machine surface, including the radial pressure and the sound power. It is worthy to mention that this magnetic vibration and noise analysis approach is suitable for nearly all DSM machines.

II. Machine Design

Fig. 1 shows the structure of the proposed dc-MSR machine, which consist of an outer rotor with 26 salient poles and an inner stator with six groups and 24 salient poles. The outer rotor is made of laminated steel which has no any PM or winding, hence very robust for intermittent operation. The inner stator accommodates both armature winding and dc-excited winding. All windings are located at six big slots, hence reducing the winding ends and shortening the flux paths.

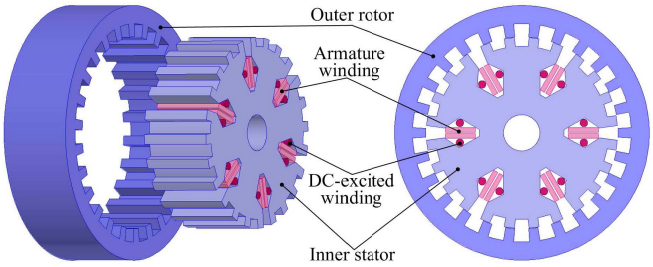

Fig. 1. Structure of proposed dc-MSR machine.

The pole-pair selection criteria of the proposed dc-MSR machine are governed by [2]

$$\begin{cases} N_{ss} = 2mk \\ N_{sp} = N_{sa} N_{ss} \\ N_{rp} = N_{sp} + 2k \end{cases} \tag{1}$$

where m is the number of phases, N_{ss} is the number of stator slots for armature windings, k is the integer, N_{sp} is the number of stator poles, N_{sa} is the number of poles per phase per armature slot, and N_{rp} is the number of rotor poles. For the proposed machine, $m = 3$, $N_{ss} = 6$, $k = 1$, $N_{sp} = 24$, $N_{sa} = 4$, and $N_{rp} = 26$. The design data of the machine is listed in Table I.

The key features of the proposed dc-MSR machine are summarized as follows.

1) The outer rotor is able to directly couple with the rotating component, such as the wind blades or EV tire rims. Also, since the machine has multipoles, it can effectively reduce the torque ripple and balance the radial magnetic attraction.
2) The machine inherently has the fault-tolerant operating capability with two sets of windings for two operation modes, namely the normal dc-excited mode and the MSR mode.

Manuscript received March 7, 2014; revised April 22, 2014 and May 12, 2014; accepted May 12, 2014. Date of current version November 18, 2014. Corresponding author: C. Liu (e-mail: chualiu@eee.hku.hk).

Color versions of one or more of the figures in this paper are available online at http://ieeexplore.ieee.org.

Digital Object Identifier 10.1109/TMAG.2014.2323706

TABLE I
MACHINE KEY DESIGN DATA

Item	Value
Outer rotor outside diameter	280.0 mm
Outer rotor inside diameter	211.2 mm
Stator outside diameter	210.0 mm
Stator inside diameter	40.0 mm
Airgap length	0.6 mm
Stack length	80.0 mm
Cross-sectional area of the conductors for the armature winding and DC winding	90 mm^2 (the armature) 170 mm^2 (the DC)
Number of rotor poles	26
Number of stator poles	24
Number of winding slots	6
Number of armature winding turns	50
Number of DC-excited winding turns	100
Number of phases	3

3) Although the number of turns of the dc winding has the double value of the armature winding, the dc winding is still sufficient and effective for current regulation [2], [3], [9].
4) The inner stator accommodates all windings, which fully utilizes its space. Also, no PMs are adopted for the machine design, which greatly reduce the machine cost.
5) The machine adopts the multitoothed structure [10], which offers the flux-modulation effect to enlarge its output torque.
6) With the dc-excited winding, the machine can fully use all torque producing zones [9], [3]. Moreover, the airgap flux density can be online regulated.

III. MAGNETIC VIBRATION ANALYSIS

A. Machine Operation Principle

The proposed machine is capable to operate in bipolar conduction mode which is similar as the conventional brushless dc (BLDC) operation principle [2], [3]. When the dc flux-linkage Ψ_{DC} is increasing, a positive rectangular current I_{BLDC} is applied to the armature winding to produce the positive torque T_{DC}. Meanwhile, a negative rectangular current $-I_{BLDC}$ is applied instead when Ψ_{DC} is decreasing and the torque produced will also be positive. The corresponding operating waveform is shown in Fig. 2. At this BLDC operation mode, each phase is conducted as 120° conduction angle. The electromagnetic torque T_{DC} can be expressed as [2], [3]

$$T_{DC} = \frac{1}{2\pi}\int_0^{2\pi}\left(i_{BLDC}\frac{d\Psi_{DC}}{d\theta}\right)d\theta = \frac{2}{3}I_{BLDC}K_{DC} \tag{2}$$

where K_{DC} is the slope of variation of Ψ_{DC}. It should also be mentioned that in this operating mode, the electromagnetic torque is mainly contributed by dc-excited component; meanwhile, the reluctance torque pulsates with zero-averaged value in each cycle [2], [3].

Because the proposed double-salient machine adopts the multitoothed structure, the radial magnetic attraction between the stator and rotor poles is more symmetrical than the conventional double-salient types. Moreover, the radial displacement of this machine is less than the PM machine owing to the strong attracting capability of PMs. The maximum radial

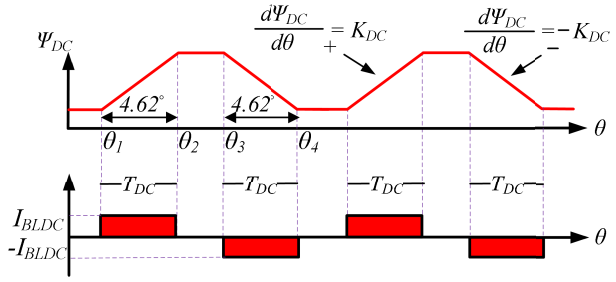

Fig. 2. Operation principle of proposed machine.

displacement caused by the magnetic vibration is set to a reasonable value of 10 μm, because the proposed machine volume is not large and is with outside diameter of 280 mm only [8]. Actually, in most cases, the radial displacement of the machine cannot reach this value.

B. Magnetic Vibration Analysis

The magnetic vibration and noise analysis of the proposed machine are based on the FEM results. So, first the TS-FEM accomplished calculating the machine radial force and torque. Then, the analytical equations are formulated to calculate the magnetic vibration parameters.

The FEM model includes three sets of equations, including the electromagnetic field equation, the armature circuit equation, and the motion equation. These equations can be referred in [9], [11], and [12].

Then, with the TS-FEM calculation results, the radial force of the machine can be obtained. Hence, all the radial-position force and pressure results can be deduced. Moreover, the values of sound power level owing to magnetic radial vibration are calculated according to the experience equation. The key equations of radial pressure P_r and sound power radial level P_s are governed by [7]

$$P_r = F_{\text{rad}}/L_a l_p \tag{3}$$
$$P_s = 4L_{\text{ax}}\sigma\rho c\pi^3 f_{\text{exc}}^2 x^2 R_o \tag{4}$$
$$\sigma = a^2/\left(1+a^2\right) \tag{5}$$
$$a = 2\pi R_o f_{\text{exc}}/c \tag{6}$$

where F_{rad} is the radial force, L_a is the axial length, l_p is the circumferential line for pressure calculation, σ and a are the coefficients, ρ is the material density, c is the traveling speed of sound in the medium, f_{exc} is the winding excitation frequency, x is the radial displacement caused by magnetic vibration (usually below 10 μm for kilowatt machine [8]), and R_o is the outer radius of machine. As derived in (3), it can be found that produced pressure is affected by the radial force and the machine volume. Thus, the radial pressure is not mainly affected by the torque density of the machine. In addition, the sound power in dB can be expressed as [7]

$$L_w = 10\log\left(2P_s/P_{\text{sref}}\right) \tag{7}$$

where $P_{\text{sref}} = 10^{-12}$ W is the sound power reference level.

Fig. 3 shows the no-load magnetic field distribution of the proposed machine with the dc-excited current of 500 A turn. As expected, the flux lines are modulated by the stator

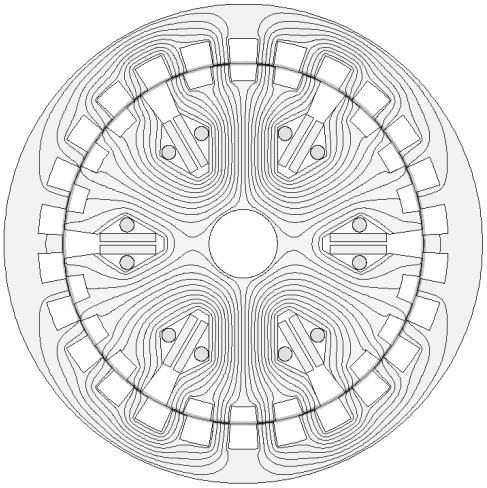

Fig. 3. Magnetic field distributions with 500 A turn.

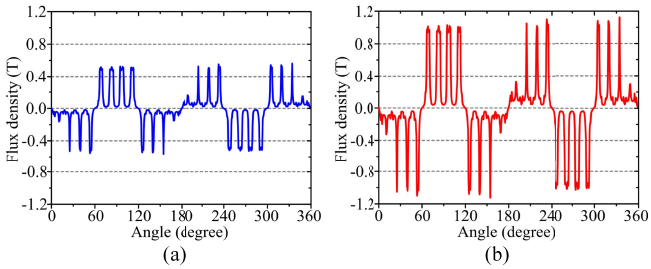

Fig. 4. Airgap flux density with different dc-excited currents. (a) With 250 A turn. (b) With 500 A turn.

multitooth and then gone through to the rotor teeth. Also, it can be seen that the flux contour is smooth and regular.

IV. Results

Performing the TS-FEM and obeying the preceding magnetic attraction equations, the machine basic performances and the corresponding magnetic vibration results can be calculated and obtained.

First, the machine basic characteristics are calculated and analyzed. Fig. 4 shows the airgap flux density with different dc-excited currents. It can be found that the airgap flux density is up to 0.54 and 1.05 T with the dc-excited current of 250 and 500 A turn, respectively. Obviously, the higher excited current is leading to the higher value of the airgap flux density. The corresponding no-load EMF waveforms are given in Fig. 5. It can be found that the EMF amplitudes are up to 90.0 and 165.0 V with the dc-excited current of 250 and 500 A turn, respectively. Hence, these results verify the validity of the machine design with the dc-excited winding for producing the magnetic field.

Second, the torque performances of the machine are calculated and discussed. Fig. 6 shows the torque-angle capability of the proposed machine under the phase armature constant current of 4, −2, and 2 A, as well as with the dc-excited current of 250 and 500 A turn. It can be found that the machine can produce the output torque up to 6.9 and 14.6 Nm with the dc-excited current of 250 and 500 A turn. Moreover, Fig. 7 shows the steady-state torque and the cogging torque under the rated conditions with the dc-excited current of

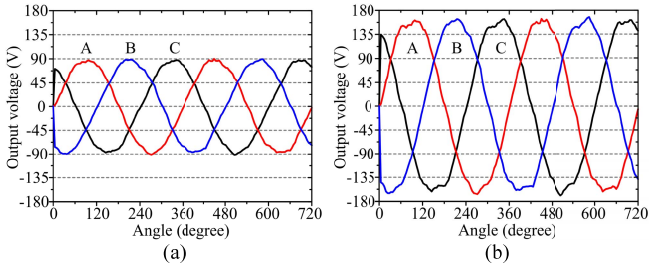

Fig. 5. No-load EMFs with different dc-excited currents. (a) With 250 A turn. (b) With 500 A turn.

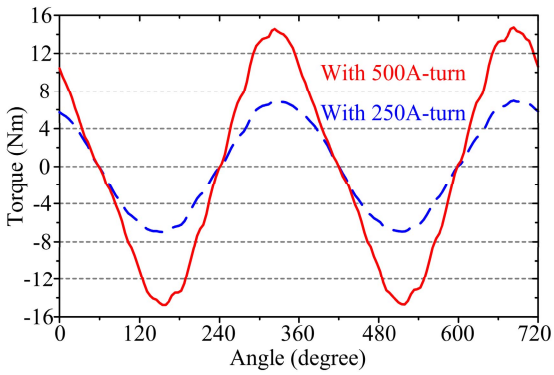

Fig. 6. Torque-angle capability with different dc-excited currents.

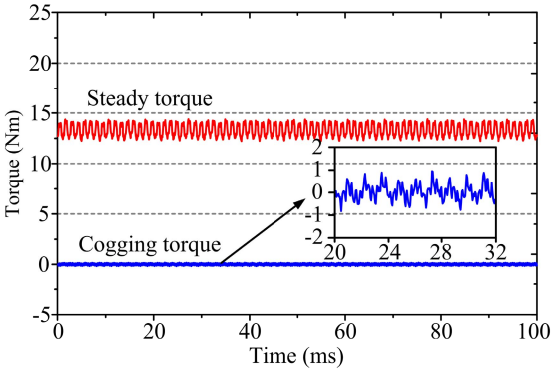

Fig. 7. Steady torque and cogging torque waveforms with the dc-excited current of 500 A turn.

500A-turn. It can be found that average steady-state torque is around 13.0 Nm and the torque ripple is only about 20.2%. Meanwhile, the maximum cogging torque is about 0.76 Nm, which is quite small and only 5.8% of its steady-state torque. The copper loss, armature winding loss, and dc-excited loss are 22.4, 28.8, and 30 W, respectively. Thus, it tells that the machine has low power loss and high efficiency up to 93.3%. The corresponding machine performances are summarized in Table II. The torque density of the proposed machine is 2.7 kNm/m^3 (2.7 Nm/L), which is about 30% (9.5 Nm/L) the double-salient PM (DSPM) machine [2]. Although the torque density of the proposed machine is lower than that of the DSPM machine, the proposed machine is able to operate at the low speed. This is the major merit of the multitoothed machine. Because of the high leakage of the flux, this machine has a low power factor of 0.38, which is expected.

Third, the magnetic vibration results are evaluated and discussed. Fig. 8 shows the radial force at the stator teeth under the rated condition. It can be found that the maximum

TABLE II
MACHINE PERFORMANCE

Item (with field current of 500 A-turn)	Value
Power	820 W
Rated speed	600 rpm
Rated current	4 A
No-load EMF amplitude	165.0 V
Maximum torque	14.6 Nm
Rated torque	13.0 Nm
Torque ripple	20.2%
Cogging torque	0.76 Nm
Core loss	22.4 W
Winding loss	58.8 W
Efficiency	93.3%

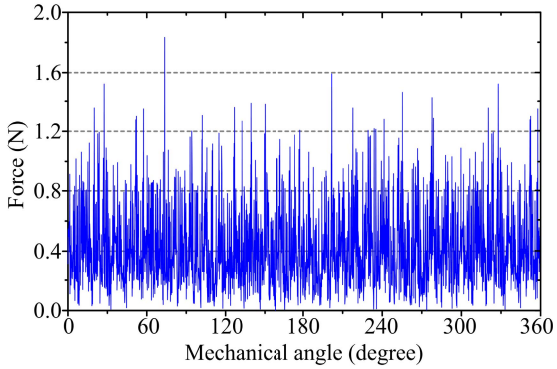

Fig. 8. Radial force at stator teeth under rated condition.

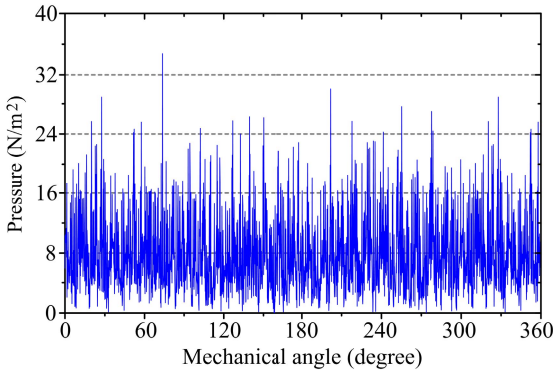

Fig. 9. Radial pressure at stator teeth under rated condition.

radial force can be up to 1.8 N and the average value is about 0.41 N. In addition, with (3), the corresponding radial pressure in the stator teeth is shown in Fig. 9. It tells that the maximum pressure is only 34.0 N/m^2 and the average value of is about 7.7 N/m^2. Thus, it indicates that the pressure in the stator teeth is not high. Also, since the difference between the radial force and pressure is the constant coefficients of L_a and L_p, they have the same contour in figures.

Moreover, Table III shows the detailed vibration results of the proposed machine at the radial direction under the rated condition. Since the machine is about 820 W, the maximum radial displacement owing to magnetic vibration is set to the reasonable value of 10 μm [8]. It indicates that the maximum noise appears at the place of machine surface. And the corresponding magnetic noise is only 71.6 dB which is quite acceptable when comparing with the conversation noise around 60.0 dB and the radio noise around 75.0 dB. Thus, this dc-MSR machine has an acceptable noise and good output torque for direct-drive application.

TABLE III
MAGNETIC VIBRATION RESULTS

Item	Value
Maximum radial displacement	10 μm
Radial force at stator teeth (maximum)	1.80 N
Radial force at stator teeth (average)	0.41 N
Radial pressure at stator teeth (maximum)	34.0 N/m^2
Radial pressure at stator teeth (average)	7.7 N/m^2
Sound power at stator teeth	1.95 W
Noise level at stator teeth	70.9 dB
Sound power at machine surface	2.60 W
Noise level at machine surface	71.6 dB
Stator and rotor material	Iron steel

V. CONCLUSION

In this paper, a new dc-MSR machine is proposed for magnetic vibration and noise analysis. The machine design and operation principle are discussed. Also, the TS-FEM is performed to calculate the machine force, torque, and other characteristics. With these results, the analytical equations are formulated to calculate the magnetic vibration parameters. The results show that proposed machine has the good torque performances and the acceptable noise effect. In addition, it is worthy to mention that this magnetic vibration and noise analysis approach are suitable for nearly all DSM machines.

ACKNOWLEDGMENT

This work was supported by the HKU Small Project Funding, Hong Kong Special Administrative Region, China, under Project 201209176143.

REFERENCES

[1] N. Radimov, N. Ben-Hail, and R. Rabinovici, "Switched reluctance machines as three-phase AC autonomous generator," *IEEE Trans. Magn.*, vol. 42, no. 11, pp. 3760–3764, Nov. 2006.
[2] C. H. T. Lee, K. T. Chau, and C. Liu, "A magnetless axial-flux machine for range-extended electric vehicles," *Energies*, vol. 7, no. 3, pp. 1483–1499 Mar. 2014.
[3] C. Liu, K. T. Chau, J. Zhong, and J. Li, "Design and analysis of a HTS brushless doubly-fed doubly-salient machine," *IEEE Trans. Appl. Supercond.*, vol. 21, no. 3, pp. 1119–1122, Jun. 2011.
[4] I. Husain, A. Radun, and J. Nairus, "Unbalanced force calculation in switched-reluctance machines," *IEEE Trans. Magn.*, vol. 36, no. 1, pp. 330–338, Jan. 2000.
[5] Y. Fan, K. T. Chau, and S. Niu, "Development of a new brushless doubly fed doubly salient machine for wind power generation," *IEEE Trans. Magn.*, vol. 42, no. 10, pp. 3455–3457, Oct. 2006.
[6] J. Li and Y. Cho, "Investigation into reduction of vibration and acoustic noise in switched reluctance motors in radial force excitation and frame transfer function aspects," *IEEE Trans. Magn.*, vol. 45, no. 10, pp. 4664–4667, Oct. 2009.
[7] P. Pillay and W. Cai, "An investigation into vibration in switched reluctance motors," *IEEE Trans. Ind. Appl.*, vol. 35, no. 3, pp. 589–596, May/Jun. 1999.
[8] R. Islam and I. Husain, "Analytical model for predicting noise and vibration in permanent-magnet synchronous motors," *IEEE Trans. Ind. Appl.*, vol. 46, no. 6, pp. 2346–2354, Nov./Dec. 2010.
[9] C. Liu, K. T. Chau, J. Z. Jiang, and S. Niu, "Comparison of stator-permanent-magnet brushless machines," *IEEE Trans. Magn.*, vol. 44, no. 11, pp. 4405–4408, Nov. 2008.
[10] J. Faiz, J. W. Finch, and H. M. B. Metwally, "A novel switched reluctance motor with multiple teeth per stator pole and comparison of such motors," *Electr. Power Syst. Res.*, vol. 34, no. 3, pp. 197–203, Sep. 1995.
[11] S. J. Salon, *Finite Element Analysis of Electrical Machines*, Boston, MA, USA: Kluwer, 1995.
[12] C. Liu, K. T. Chau, and Z. Zhang, "Novel design of double-stator single-rotor magnetic-geared machines," *IEEE Trans. Magn.*, vol. 48, no. 11, pp. 4180–4183, Nov. 2012.